JACS
JOURNAL OF THE AMERICAN CHEMICAL SOCIETY

ARTICLE

pubs.acs.org/JACS

Synthetic Chemoselective Rewiring of Cell Surfaces: Generation of Three-Dimensional Tissue Structures

Debjit Dutta, Abigail Pulsipher, Wei Luo, and Muhammad N. Yousaf*

Department of Chemistry and Carolina Center for Genome Science, University of North Carolina at Chapel Hill, Chapel Hill, North Carolina 27599-3290, United States

Supporting Information

ABSTRACT: Proper cell−cell communication through physical contact is crucial for a range of fundamental biological processes including, cell proliferation, migration, differentiation, and apoptosis and for the correct function of organs and other multicellular tissues. The spatial and temporal arrangements of these cellular interactions *in vivo* are dynamic and lead to higher-order function that is extremely difficult to recapitulate *in vitro*. The development of three-dimensional (3D), *in vitro* model systems to investigate these complex, *in vivo* interconnectivities would generate novel methods to study the biochemical signaling of these processes, as well as provide platforms for tissue engineering technologies. Herein, we develop and employ a strategy to induce specific and stable cell−cell contacts in 3D through chemoselective cell-surface engineering based on liposome delivery and fusion to display bio-orthogonal functional groups from cell membranes. This strategy uses liposome fusion for the delivery of ketone or oxyamine groups to different populations of cells for subsequent cell assembly via oxime ligation. We demonstrate how this method can be used for several applications including, the delivery of reagents to cells for fluorescent labeling and cell-surface engineering, the formation of small, 3D spheroid cell assemblies, and the generation of large and dense, 3D multilayered tissue-like structures for tissue engineering applications.

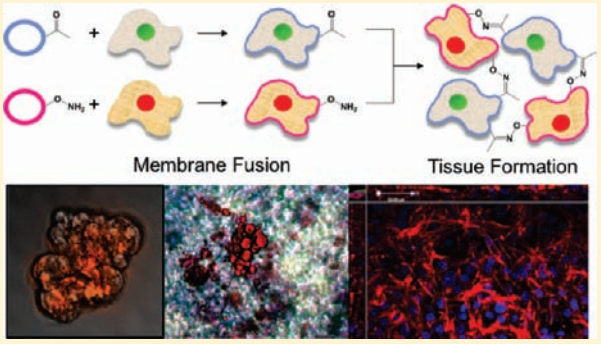

INTRODUCTION

Cells that make up tissues and organs exist and communicate within a complex, three-dimensional (3D) environment. The spatial orientation and distribution of extracellular matrix (ECM) components directly influences the manner in which cells receive, integrate, and respond to a range of input signals.[1] As such, cellular interactions with ECM molecules and/or other cells have been extensively investigated for fundamental studies in development, cell motility, differentiation, apoptosis, paracrine signaling, and applications in tissue engineering.[2,3] There has been tremendous effort toward the design and fabrication of 3D scaffolds that mimic ECM properties and induce tissue formation *in vitro*, utilizing various biomaterials, biodegradable polymers,[4] collagen,[5] and hydrogels.[6,7] Among the major challenges facing the use of these technologies for tissue engineering are the abilities to force contact between multiple cell types in 3D to control the spatial and temporal arrangement of cellular interactions and tailor and mold the biomaterial to recapitulate the 3D, *in vivo* environment under laboratory constraints. Without the use of engineered scaffolds in culture, most cells are unable to form the necessary higher-order 3D structure required for the anatomical mimicry of tissue and are limited to random migration, generating two-dimensional (2D) monolayers. As a result, several approaches, including the use of dielectrophoretic forces,[8,9] laser-guided writing,[10−12] surface manipulation,[13] and a number of lithographic printing techniques[14−17] have been integrated with 3D scaffold designs to produce multitype cellular arrays[9,11,17,18] or 3D cell clusters or spheroids.[7,8,13] In a recent study, 3D aggregates consisting of multiple cell types were formed within a hydrogel matrix through DNA hybridization after cell surfaces were engineered with complementary short oligonucleotides via a metabolic labeling approach.[7] However, for some applications, the presentation of cell-surface DNA may not be stable for extended time periods in cell culture or *in vivo*.

Cell-surface engineering methodologies have primarily been of interest in molecular biology. As such, biosynthetic approaches have been employed to introduce different functional groups on cell surfaces. In a pioneering study, an unnatural derivative of *N*-acetyl-mannosamine, which bears a ketone group, was converted to the corresponding sialic acid and metabolically incorporated onto cell-surface oligosaccharides, resulting in the cell surface display of ketone groups.[19] However, metabolic or genetic methods may alter many of the biochemical pathways required for normal cell function and not all cell lines possess this metabolic machinery. Thus, there is a growing demand for general tools that can provide simple alternatives to the complex genetic and biosynthetic methods. Other approaches to cell-surface

Received: March 11, 2011
Published: May 11, 2011

ACS Publications © 2011 American Chemical Society

dx.doi.org/10.1021/ja2022569 | *J. Am. Chem. Soc.* 2011, 133, 8704–8713

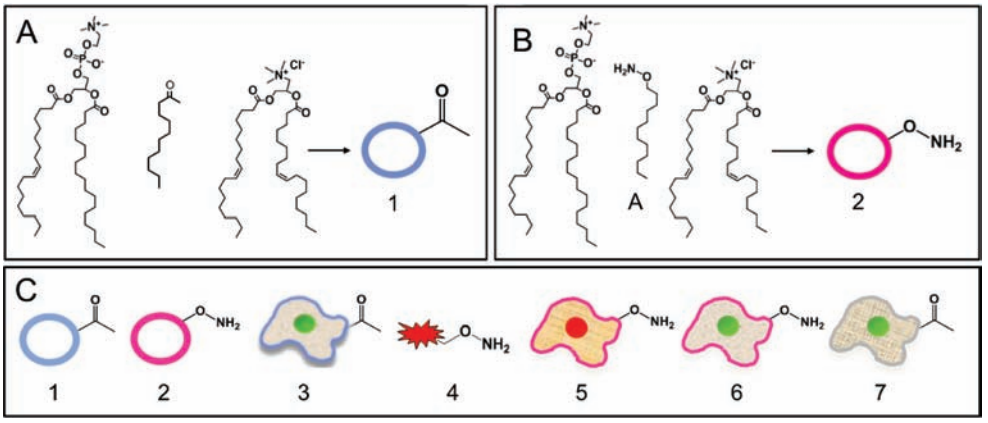

Figure 1. General schematic of liposome preparation for cell-surface tailoring. (A) Dodecanone molecules were incorporated into neutral, egg palmitoyl-oleoyl phosphatidylcholine (POPC) and cationic, 1,2-dioleoyl-3-trimethylammonium-propane (DOTAP) at a ratio of 5:93:2 to form ketone-presenting liposomes (**1**). (B) *O*-Dodecyloxyamine (**A**) molecules were incorporated into POPC and DOTAP at a ratio of 5:93:2 to form oxyamine-presenting liposomes (**2**). (C) List of liposomes, molecules, and cells used in this study: (**1**) ketone-functionalized liposomes; (**2**) oxyamine-functionalized liposomes; (**3**) ketone-functionalized Swiss 3T3 albino fbs; (**4**) rhodamine-functionalized oxyamine (rhod-oxyamine); (**5**) m-cherry labeled, oxyamine-functionalized rat2 fbs; (**6**) oxyamine-functionalized Swiss 3T3 albino fbs; and (**7**) ketone-functionalized hMSCs.

engineering have also been undertaken to incorporate a functional group into a target biomolecule, such as an endogenous protein, utilizing a cell's biosynthetic machinery.[20,21] These strategies aim to produce a site that can then be covalently modified with its delivered counterpart or probe. However, most of these protein-based tags are large and bulky and become problematic when interacting with the other glycans and biomolecules on the cell suface.[22,23] Additionally, the perturbation of cellular physiology with biomolecules at the cell surface may result in the interference of significant biochemical pathways or cellular functions.[24,25] Thus, a methodology that combines cell-surface modification, without the use of molecular biology techniques or biomolecules, and a simple, stable bio-orthogonal conjugation bottom-up approach that is capable of directing tissue formation would greatly benefit a range of medical applications such as wound healing and burn treatment.

Herein, we develop and employ a novel strategy to induce specific and stable cell−cell contacts through chemoselective cell-surface engineering based on liposome delivery and fusion of bio-orthogonal functional groups to cell membranes.[26] Our liposome-cell membrane methodology was inspired by the work of Wilson et al.[27] and Csiszar et al.[28] who reported a noncovalent cell-surface engineering strategy via cationic graft copolymer adsorption and a fluorescent cell labeling technique via cationic and aromatic lipid fusion, respectively. Thus, we incorporated a cationic lipid to initiate membrane fusion and adsorption to the cell surface. This strategy enables the presentation of bio-orthogonal ketone and oxyamine molecules from cell surfaces for subsequent chemoselective oxime ligation. No proteins or large biomolecules are used in this strategy, and therefore, cellular physiology is not perturbed. We demonstrate how this method may be used in several applications, including the delivery of reagents to cell surfaces, formation of 3D spheroid assemblies of cells with controlled interconnectivity, and patterned multilayered cell tissues. Furthermore, 3D multilayered stem cell and fibroblast (fb) co-cultures were generated, and differentiation was induced to form tissue-like structures of adipocytes and fbs. To our knowledge, this is the first report utilizing tailored liposomes to modify a living cells surface through membrane fusion for subsequent bio-orthogonal tailoring to generate 3D tissue-like structures.

RESULTS AND DISCUSSION

Vesicle fusion to cell membranes was directed through the use of a cationic lipid and a molecular recognition pair for chemoselective ligation toward the goal of rewiring cell adhesion to generate 3D multilayers of cells. Vesicles were tailored with ketone (dodecanone) or oxyamine (*O*-dodecyloxyamine) molecules, a neutral lipid, egg palmitoyl-oleoyl phosphatidylcholine (POPC), and a cationic lipid, 1,2-dioleoyl-3-trimethylammonium-propane (DOTAP). The resulting two vesicle populations were then integrated with mammalian cells in culture for applications in small molecule delivery, cell-surface modification, and tissue engineering. By employing this membrane tailoring strategy, the assembly of 3D spheroid clusters and tissue-like structures were directed after culturing two cell populations functionalized with oxyamine- and ketone-containing groups. Because this method is general, bio-orthogonal, chemically stable (oxime bond), and noncytotoxic, patterned multilayered tissue-like structures of different geometric shapes could also be fabricated without the use of 3D scaffolds to confine the cell populations. We also show that this method has promising use in stem cell transplantation by co-culturing human mesenchymal stem cells (hMSCs) with fibroblasts (fbs) and inducing adipocyte differentiation while in a 3D multilayered tissue-like structure.

For membrane fusion studies, dodecanone and *O*-dodecyloxyamine (**A**) were incorporated separately into neutral POPC and cationic DOTAP lipids at a ratio of 5:93:2 (Figure 1A,B). The alkane-tethered ketone and oxyamine molecules (**A**) spontaneously insert themselves into the vesicles during syntheses.[29] The cationic lipid, DOTAP, was added to enhance membrane fusion via electrostatic destabilization due to the negatively charged cell membrane and subsequent lipid component display at the cell surface. A minimum 2% DOTAP amount was determined and optimized for liposome-cell fusion initiation by investigating concentrations that ranged from 0.5% to 5%. The POPC concentrations were varied accordingly, while maintaining the ketone at 5%. An oxyamine-tethered rhodamine (rhod-oxyamine, **4**) (7 mM in H_2O, 100 μL added to 4 mL, 2 h) was then conjugated to cell surfaces after liposome fusion, and the fluorescence intensities of each lipid ratio were compared.

dx.doi.org/10.1021/ja2022569 |*J. Am. Chem. Soc.* 2011, 133, 8704–8713

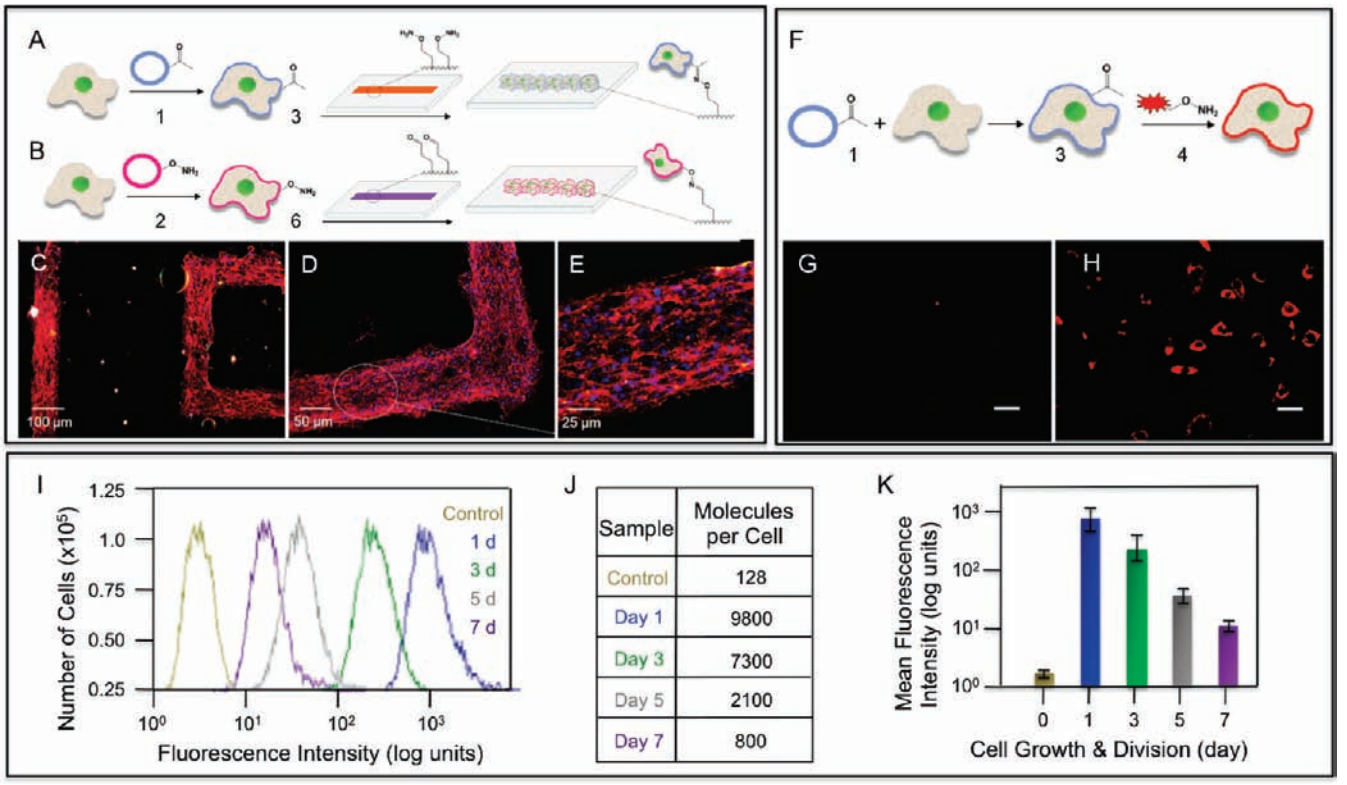

Figure 2. Liposome-cell fusion characterization by cell patterning, fluorescence microscopy, and fluorescence-activated cell sorting (FACS) analysis. A schematic and images of cells, rewired to adhere to patterned, synthetic ligands are shown in panels A−E. Cells were cultured separately with (A) ketone- (**1**) or (B) oxyamine- (**2**) containing liposomes and then seeded on patterned surfaces displaying the complementary oxime conjugation group. (C) Ketone-functionalized cells (**3**) adhered to patterned surfaces presenting oxyamine groups, while (D) oxyamine-functionalized cells (**6**) adhered to patterned surfaces presenting aldehyde groups. (E) A higher magnification image of the cells in panel D is shown. The cells in panels C−E were stained with DAPI (blue, nucleus), phalloidin (red, actin), and Cy-2 (green, anti-vinculin). A general schematic and images for cell-surface tailoring using liposome fusion and chemoselective oxime chemistry are demonstrated in panels F−H. (F) Ketone-functionalized lipid vesicles (**1**) were added and fused with fbs, displaying ketones from the cell surface (**3**). Addition of rhod-oxyamine (**4**) resulted in chemoselective oxime formation and the fluorescent labeling of fbs. The images displayed represent (G) control fbs, where liposomes not displaying ketones were fused to the membrane, followed by rhod-oxyamine addition (**4**, 7 mM in H_2O, 2 h), and no fluorescence was observed and (F) fluorescently labeled cells after ketone-functionalized liposomes (**1**) were fused to fbs and incubated with rhod-oxyamine (**4**, 7 mM in H_2O, 2 h. The scale bars in panels G and H represent 40 μm. The determination of ketone molecules per cell by flow cytomtery is shown. Fbs were cultured with (**1**) or without (control) ketone-containing liposomes for 1, 3, 5, and 7 days. The fbs (**3**) were then reacted with hydrazide-conjugated biotin, followed by fluorescein-labeled streptavidin. Fbs were then tested against a standard bead ($\sim 10^7$ beads/mL) with known fluorescein molecule density. Approximately 10^5 cells were counted for all samples. Samples were run in triplicate, and the mean fluorescence intensity values are displayed ± RSD. (I) FACS data relating the number of cells counted ($\sim 10^5$) as a function of fluorescence intensity are shown and labeled as control (without ketone) and days 1, 3, 5, and 7 (with ketone). Fluorescence was observed for all ketone-displaying populations with a decrease from 1 to 7 days, indicating that the ketone group is carried through cell growth and division. (J) The number of fluorescein molecules was calculated by comparing the relative mean intensity to a standard bead with known fluorescein molecule density. The numbers of ketone molecules per cell, as well as the control, are listed, showing a decrease in density on the cell surface over time. (K) The relationship between the mean fluorescence intensity and the number of days incubated with ketone-containing liposomes is shown. As cells grow and divide over the course of 7 days, the ketone is carried through.

From 2% to 5% DOTAP, the fluorescence intensities were almost identical, indicating that 2% DOTAP is sufficient to initiate fusion. Our general fusion strategy to generate 3D tissue-like structures is represented in Figure 3A. When cells are incubated with ketone- (**1**) or oyamine- (**2**) containing liposomes, membrane fusion occurs, resulting in the presentation of ketone and oyamine groups from cell surfaces (**3**, **7**, and **5**, **6**, respectively). When these cell populations are cultured together, interconnected, 3D tissue-like structures form, mediated through chemoselective oxime conjugation. These stable tissue structures can be generated in solution or on a solid support.

Rewiring Cell Adhesion. The ability to adhere cells to a variety of materials through a simple bio-orthogonal approach that does not rely on proteins or complex ligands enables novel ways to manipulate cells and modify biomaterials for a range of biotechnological and tissue engineering applications. Therefore, we extended our liposome fusion strategy to rewire cells to adhere to materials presenting bio-orthogonal, complementary synthetic ligands (Figure 2A−E). Two cell populations were cultured separately with ketone- (**1**) or oxyamine- (**2**) containing liposomes and were then seeded on patterned surfaces displaying either oxyamine or aldehyde groups, respectively. Employing previously developed self-assembled monolayer (SAM) technologies, surfaces were patterned via a microfluidics to present either 10% oxyamine[31] or aldehyde[32] and 90% tetra(ethylene)glycol (EG_4) functional groups (Figure 2, panels A and B, respectively). The remaining, unpatterned region was backfilled to present EG_4 terminal groups, which are known to resist nonspecific protein

dx.doi.org/10.1021/ja2022569 |*J. Am. Chem. Soc.* 2011, 133, 8704–8713

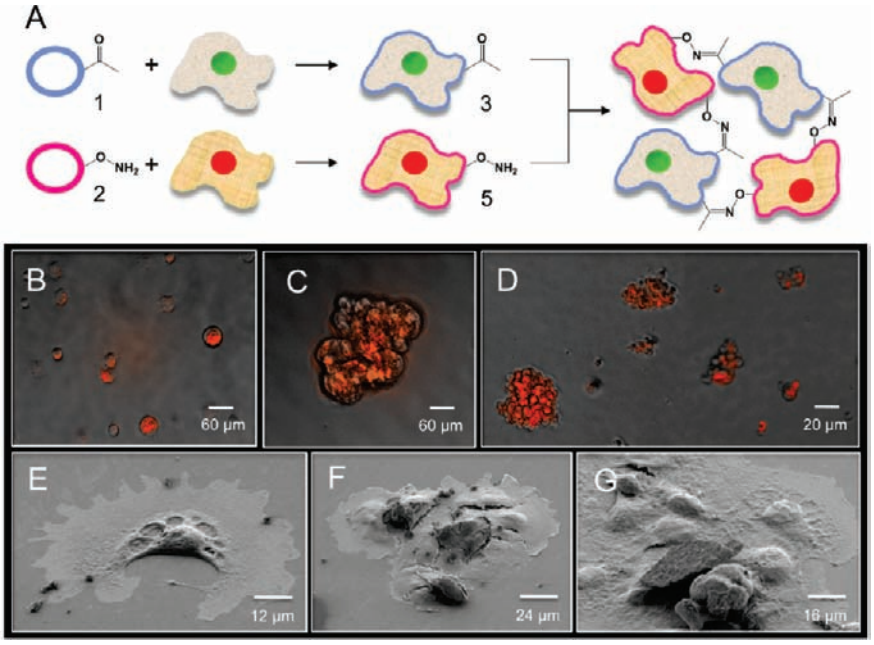

Figure 3. Fluorescent, phase contrast, and scanning electron micrographs (SEM) describing 3D spheroid formation via liposome fusion and chemoselective cell-surface tailoring. Two fb populations were cultured separately with ketone- (**1**) or oxyamine- (**2**) containing liposomes, resulting in membrane fusion and subsequent tethering of ketones and oxyamines from the cell surface. The oxyamine-tethered rat2 fibroblasts (**5**) contained a fluorescent m-cherry nuclear label. The ketone-presenting Swiss albino 3T3 fibroblasts (**3**) were not fluorescently labeled. (A) Two fibroblast populations were cultured separately with ketone- (**1**) or oxyamine- (**2**) containing liposomes. Because of the presence of a positively charged liposome, fusion occurred, producing ketone- (**3**) and oxyamine- (**5**) tethered cells. Upon mixing these cell populations, clustering and tissue-like formation, based on chemoselective oxime conjugation, occurred. (B) Control experiments (overlay image) demonstrate no spheroid formation for cells that did not contain either ketone or oxyamine groups. (C and D) However, when two cell populations displaying ketone (**3**) and oxyamine (**5**) recognition groups are mixed, interconnected spheroid assemblies form (overlay images). (E−G) Representative SEM images of (E) control cells and (E and F) spheroid assemblies, as described above, are displayed. For all spheroid assemblies depicted, cell populations were mixed and cultured together for 3 h before imaging at $\sim 10^4$ cells/mL.

adsorption and cell attachment.[33] Upon seeding cells presenting ketone (**3**) or oxyamine (**6**) groups to the complementary surfaces, an interfacial oxime reaction occurred and cells adhered, spread, and proliferated in the patterned regions (Figure 2C−E). However, untreated cells and cells cultured with liposomes, not containing the key functional groups, did not attach to the surface. This strategy allows for a bottom-up, bio-orthogonal synthetic approach to rewire how cells adhere to materials and does not require genetic manipulations of cells.

Cell-Surface Labeling. Using bio-orthogonal approaches to label specific subcellular organelles and cell-surface membranes is of great interest to research fields ranging from chemical biology and tissue engineering to drug delivery. A number of pioneering approaches involving Staudinger ligation[24,34] and click chemistry[20] have been employed for specific covalent and noncovalent cell-surface engineering applications. In this report, we use oxime chemistry to tailor and fluorescently label the cell surface via a novel liposome-cell fusion method. Ketone-functionalized vesicles (**1**) were delivered to fibroblasts in culture (Figure 2F). After 4 h of incubation, the liposomes fused to the cell membranes, causing the cell surface to be decorated with ketone groups (**3**). These ketones remain dormant until reaction with rhod-oxyamine (**4**, 7 mM in H_2O, 2 h) after which the cells became fluorescent, as shown in the fluorescent image in Figure 2H. A control was performed where nonfunctionalized liposomes were added to cells in culture (4 h), followed by subsequent addition of rhod-oxyamine (**4**, 7 mM in H_2O, 2 h). The fluorescent image indicated that the reaction and labeling did not occur without the proper oxime recognition pair (Figure 2G). Furthermore, under these conditions, we observed no changes in cell behavior upon liposome fusion to cells. This observation is a very important feature for future *in vivo* applications for cell labeling and targeting via pulse and chase type methods. Thus, by combining liposome fusion and oxime chemistry, we were able to tailor the cell surface with either ketone groups or oxyamine groups, which may act as chemoselective cell-surface receptors for a range of small molecules, ligands, biomolecules, and nanoparticles.

Flow Cytometry. After conducting the above liposome-cell fusion characterization experiments, we hypothesized that cell proliferation of the liposome-fused cell tissue carries unreacted ketone or oxyamine groups on the cell membranes. This hypothesis was further supported by flow cytometry in conducting FACS analysis (Figure 2I−K). Ketone-functionalized cells (**1**) were reacted with hydrazide-conjugated biotin (3 mM in CBS, 1 h), followed by fluorescein-tethered streptavidin (1 mM in CBS, 1 h), and the fluorescence intensity was compared to a bead of known fluorescein density and control cells (without ketone groups).[35] The approximate number of ketone and oxyamine molecules displayed from the cell surface after membrane fusion (12 h), as well as throughout cell growth and division (3, 5, and 7 days in culture), was then tabulated. FACS showed that approximately 9800 ketone or oxyamine molecules were imbedded into the cell surface after 12 h of liposome incubation (Figure 2J). Further culturing these cells indicated a decrease

dx.doi.org/10.1021/ja2022569 |*J. Am. Chem. Soc.* 2011, 133, 8704–8713

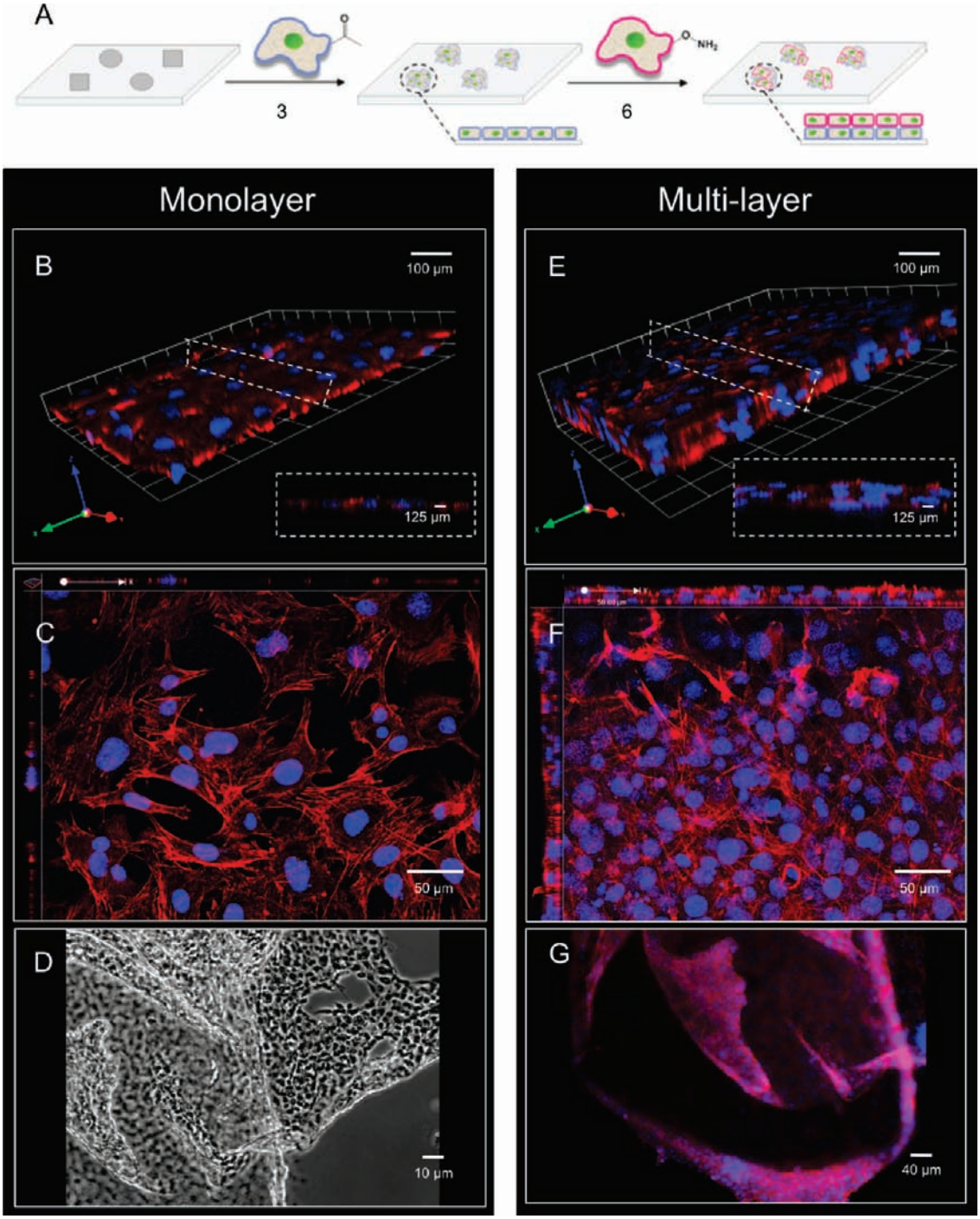

Figure 4. General schematic and images of oxime-mediated, 3D tissue-like structure formation with controlled interconnectivity. (A) Ketone- (**1**) and oxyamine- (**2**) containing liposomes were added to two separate fb populations, resulting in membrane fusion and subsequent presentation of the ketone (**3**) and oxyamine (**6**) groups from cell surfaces. Culturing these cells on substrates, alternating cell population seeding layer-by-layer, gave rise to multilayered, tissue-like cell sheets through stable oxime chemistry. (B) A 3D reconstruction and (C) confocal micrograph showing only a monolayer of cells after oxyamine-presenting cells (**6**) were cultured with adhered nonfunctionalized cells. (E) A 3D reconstruction and (F) confocal micrograph of multiple cell layers after oxyamine-presenting cells (**6**) were added to substrates presenting ketone-containing cells (**3**). (D and G) Intact, 3D multilayered cell sheets can be removed from the surface by gentle agitation as displayed by brightfield and fluorescent images. The insets in panels B and E show a *z*-plane cross section that indicates the thickness of the cell layers. Cells were stained with DAPI (blue, nucleus) and phalloidin (red, actin).

in available molecules from 3, 5, and 7 days with 7300, 2100, and 800 molecules per cell, respectively (Figure 2J). Fluorescence was still detected, although not as intense, after 7 days of cell culture, indicating that ketone and oxyamine groups were carried through cell division. Control cells (without ketone groups) that were incubated with hydrazide-biotin and fluorescein-tethered streptavidin demonstrated little to no fluorescence (Figure 2I–K).

dx.doi.org/10.1021/ja2022569 |*J. Am. Chem. Soc.* 2011, 133, 8704–8713

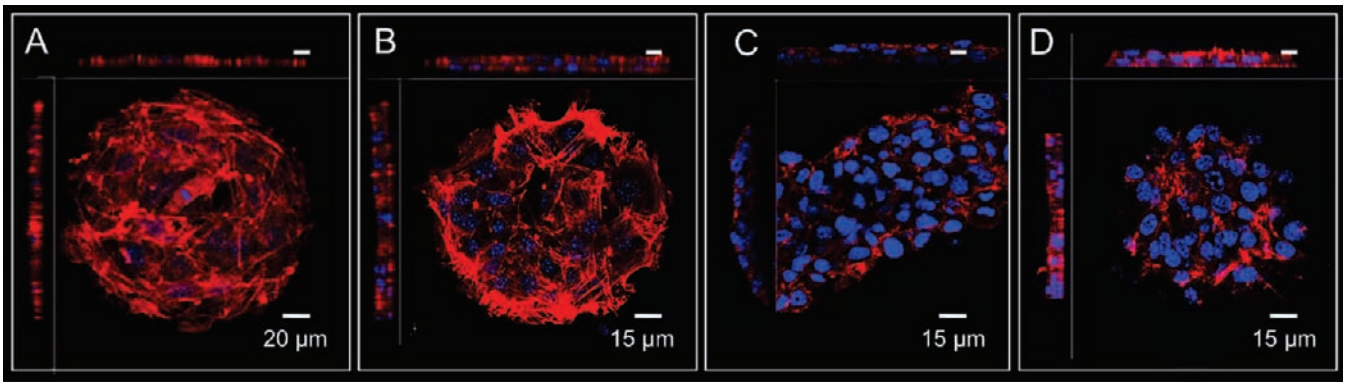

Figure 5. Confocal images representing 2D monolayer and 3D multilayered tissue-like structures of fbs with spatial control. (A) A circular, 2D monolayer of fbs (control) result after ketone-functionalized fbs (**3**) and fbs (not functionalized with oxyamines) are patterned on a circular, microcontact printed region, presenting fibronectin and allowed to grow for 5 days. (B−D) Fbs, functionalized with ketone groups (**3**) were seeded onto microcontact printed regions containing fibronectin and allowed to grow for 2 days. Fbs, functionalized with oxyamine groups (**6**) were then seeded and allowed to grow for 2−3 more days. Confocal images demonstrating 3D tissue formation in (B) circle, (C) bar, and (D) square geometries are depicted. The corresponding *z*-plane cross sections that indicate the thickness of the cell layers are shown as an inset; scale bars represent 30 μm. Cells were stained with DAPI (blue, nucleus) and phalloidin (red, actin).

3D Spheroid Assembly. The ability to generate multicellular connected tissues of multiple cell types *in vitro* is crucial for studying the complex interplay of cells in a range of organs *in vivo* and for developing strategies for synthetic tissue transplantation. With varying successes, a number of current strategies to generate 3D cell connections rely on forcing mixed cell populations into complex microfabricated wells or vessels. Therefore, we extended this liposome fusion, oxime-based strategy to generate 3D spheroid assemblies of interconnected cells using two different cell-type populations (Figure 3). The oxyamine-presenting rat2 fbs (**5**) contained a nuclear m-cherry fluorescent label so that the cell clustering to nonfluorescent ketone-tethered cells (**3**) could be easily observed. During a 3-h period of mixed-culturing ($\sim 10^4$ cells/mL) in solution, cells formed spheroid structures due to the presence of complementary recognition groups (Figure 3C,D). Furthermore, when oxyamine-presenting fbs (**5**) were cultured with control fbs (cells not functionalized with ketone groups), spheroid assembly did not occur (Figure 3B). Studies were also performed to test whether spheroid size and cell composition could be controlled (Supporting Information, Figure S1A−D). Ketone-presenting hMSCs (**7**) were co-cultured with oxyamine-functionalized fbs (**6**) for 1, 2, 3, and 5 h. After 1 h, clusters comprised only of a few cells were observed. As the co-culturing duration was increased, larger spheroid structures were observed. Notably, control experiments were performed simultaneously to ensure that spheroid generation was being directed through chemoselective oxime conjugation. Shown as insets in Figure S1A−D, tissue structure formation did not occur without the proper complementary pair displayed from cell surfaces, regardless of the mixing duration (1−5 h). Thus, size and composition of 3D cell assemblies in solution could be controlled, showing great promise for applications in stem cell transplantation and regenerative medicine.

Spheroid formation was also characterized by scanning electron microscopy (SEM) (Figure 3E−G and Figure S2). Cells functionalized with oxyamine (**6**) and ketone (**3**) groups were able to generate clusters when mixed in solution, as displayed in Figure 3F,G (Supporting Information, Figure S2). However, spheroid assemblies were not observed when ketone-presenting fbs were reacted with nonfunctionalized cells; fbs spread out on the surface, migrated, but remained alone (Figure 3E). Notably, cells were able to form stable, interconnected 3D structures in solution simply upon mixing two tailored cell populations. Currently, methods to generate these structures require the support of a 3D hydrogel matrix and/or assisted assembly through an external stimulus.[5,7−9,13]

3D Multilayered Tissues. In addition to forming small, 3D cell clusters or spheroid structures in solution, this strategy may be employed to direct larger, dense 3D tissue-like networks on a surface with geometric control. We used full substrates (Figure 4), as well as surfaces that were patterned with cell adhesive and nonadhesive regions to generate multilayered sheets and patterned tissue structures (Figure 5), respectively.[30] Ketone- (**1**) and oxyamine- (**2**) tailored liposomes were cultured with separate fb populations, resulting in membrane fusion and subsequent presentation of chemoselective sites for oxime conjugation from the surface (**3** and **6**, respectively) (Figure 4A). Culturing these groups on a solid support ($\sim 10^5$ cells/mL) and in a layer-by-layer deposition manner gave rise to multilayered, tissue-like cell sheets, which were characterized by confocal microscopy, as shown in Figure 4E,F. Fbs naturally only form a single monolayer once they become contact-inhibited. However, we have successfully induced fb−fb clustering though oxime-mediated, cell-surface engineering based on liposome fusion.

To ensure that oxime chemistry was aiding in the formation of 3D tissue-like structures, several control experiments were performed. Cells that did not present ketone or oxyamine functionality were seeded onto separate surfaces. A second cell population presenting oxyamine (**6**) or ketone (**3**) groups from the cell surface was added, resulting in the formation of only a 2D monolayer of cells (Figure 4B,C). Similarly, two different cell populations that were tethered with oxyamine (**6**) groups were mixed together, and only a 2D monolayer was generated after 4 days of culture. The same results were observed after culturing two different ketone-functionalized cell populations (**3**) for 4 days. These results further support our hypothesis that multilayered cell interconnectivity is driven by complementary, oxime chemistry. We also extended this strategy toward the generation of 3D multilayered co-cultures with hMSCs and fbs

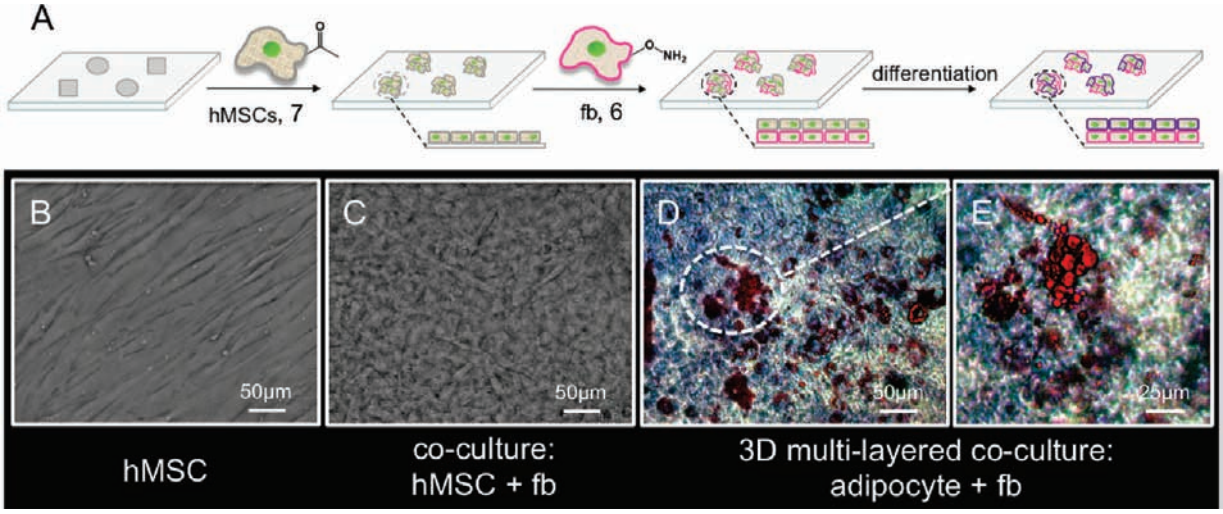

Figure 6. General schematic and brightfield images representing oxime-mediated, 3D tissue-like structure formation with hMSC/fb co-cultures and subsequent induced adipocyte differentiation to generate 3D adipocyte/fb co-culture structures. (A) Ketone-tethered hMSCs (**7**) were seeded onto a surface, followed by the addition of oxyamine-functionalized fbs (**6**). The co-culture was allowed to grow and divide for 3 days at which point, adipogenic differentiation was induced with the addition of the appropriate media. This resulted in a 3D multilayer of adipocytes and fb. (B) A confluent 2D monolayer of ketone-presenting hMSCs is represented. (C) A brightfield image displaying a 3D multilayer co-culture of hMSCs (**7**) and oxyamine-functionalized fbs (**6**) is shown. (D) Adipogenic differentiation was induced with media resulting in 3D multilayered adipocyte and fb co-culture structures, represented by low and (E) high-resolution brightfield images (after 10 days in culture). Adipocytes were stained with Oil Red O (lipid vacuoles) and Harris Hemotoxylin (nucleus).

(Supporting Information, Figure S3). Ketone-functionalized hMSCs (**7**) were first cultured on a substrate ($\sim 10^5$ cells/mL), and stem cells were allowed to spread out and grow for 2 days. Oxyamine-presenting fbs (**6**) were then added ($\sim 10^5$ cells/mL) and co-cultured for an additional 2 days. As shown by the confocal images in Figure S3B,C, 3D multilayered cell sheets (4 layers) were formed. The proper controls were conducted; without the oxime pair, only a 2D monolayer of stem cells and fbs was formed (Supporting Information, Figure S3A).

3D Tissue Release and Cell Viability. During multilayer culture, it was possible to control the release of the tissues from the surface with gentle agitation (Figure 4D,G). The ability to release tissue after surface-supported growth *in vitro* shows great potential for applications in tissue engineering and cellular transplantation. Cell viability was also tested for 3D spheroid and multilayered structures of fbs and hMSC/fb co-cultures using the trypan blue assay (Supporting Information, Figure S4).[35] After spheroid (1, 2, 3, and 5 h of mixing in solution) and multilayer (3, 5, and 7 days on a surface) formation, cells were incubated with trypan blue (0.4%, 2 min). Viability was 100% for all cells in the spheroid assemblies (1−5 h) and multilayer structure at day 3. After 5 and 7 days of multilayer generation, cells showed an approximate viability of 91% and 84%, respectively. The blue intensity (fluorescence false colored for enhanced visualization) was compared to a control cell population by linescan analysis (Supporting Information, Figure S4). The control cells were cultured for 7 days to generate 3D multilayers and were then fixed. Trypan blue was allowed to react for 2 min, followed by imaging and quantification. Overall, the viability of cells in conducting membrane fusion to generate 3D tissue-like structures in solution and on a solid support is high. Therefore, this method may be very useful for applications in tissue engineering and stem cell transplantation.

3D Tissue Patches with Geometrical Control. We further demonstrated spatial control by generating a number of 3D multicellular micropatterns. Microcontact printing[30] was used to produce a variety of patterns and geometries on a gold substrate. Employing SAM and microfabrication technologies, hexadecanethiol (1 mM in EtOH) was printed on a gold surface. The surface was then backfilled with EG_4 (1 mM in EtOH, 16 h) to render the remaining regions inert to nonspecific protein absorption. Fibronetin, a cell-adhesive protein was then added (10 mg/mL in CBS, 2 h), adhering only to the hydrophobic, patterned areas. As shown by the confocal image in Figure 5A, only a 2D, circular cell pattern arises after ketone-presenting fbs (**3**) were cultured with fbs, not functionalized with oxyamine molecules. However, when liposome fusion occurs to display complementary ketone and oxyamine groups from cell surfaces (**3** and **6**, respectively), multilayered 3D cell patterns were formed (Figure 5B−D). Circular, bar, and square circular tissue-like structures are depicted in Figure 5B−D. The ability to generate 3D tissues with controlled geometry would find great use in tissue transplantation, in which specifically tailored patches are required.

3D Stem Cell Co-cultures with Induced Adipocyte Differentiation. We explored the general use of this liposome fusion method, delivered ketone and oxyamine groups to different cell lines, and demonstrated that 3D spheroid and multilayer can be generated using co-cultures of hMSCs and fbs (Supporting Information, Figures S1 and S3, respectively). We next extended our methodology toward stem cell differentiation to determine whether 3D multilayered co-cultures could be induced to generate tissues of differentiated hMSCs and fbs. As shown in Figure 6A, ketone-functionalized hMSCs (**7**) were first cultured on a substrate for 3 days, producing a 2D monolayer of cells (Figure 6B). Oxyamine-tethered fbs (**6**) were then co-cultured with the hMSCs, and the cells were allowed to grow and proliferate for 2 days (Figure 6C). Adipogenic induction media was then added, the 3D multilayered coculture was stained for nuclei (purple) and lipid vacuoles (red), which are characteristic

dx.doi.org/10.1021/ja2022569 |*J. Am. Chem. Soc.* 2011, 133, 8704–8713

of adipocytes (fat cells). The phase contrast images in Figure 6D, E demonstrate the successful generation of tissue-like structures, comprising induced adipocytes and fbs. The ability to co-culture stem cells with many other cell types and induce differentiation shows great promise in the field of regenerative medicine and stem cell transplantation.

CONCLUSION

In this study, we developed a simple liposome delivery and fusion method to display ketone or oxyamine functional groups from cell surfaces for applications in bio-orthogonal ligand conjugation, rewiring cell adhesion, and the generation of stable, 3D spheroid assemblies and multilayered tissue-like structures. This strategy may have diverse applications in the field of tissue engineering and regenerative medicine, from growing biocompatible tissues and organs *in vitro* to their cellular transplantation *in vivo*.[36,37] For example, assembled tissue patches with geometrically defined shape can be grown in culture and transplanted or grafted to specific locations.[38] Furthermore, this strategy may allow for time-lapse observation of cell movement *in vivo* by using a pulse (delivery of labeled cells via liposome fusion), followed by a chase (bio-orthogonal reagent to target only the labeled cells). When applied *in vivo*, this method may allow for the monitoring of many spatiotemporal developmental events and tumor metastasis. Since the liposome fusion method is general, many other types of chemistries in a single liposome can be delivered to the membrane surface simultaneously. For example, liposomes containing ketones, alkynes, dienes, azides, hydrazides, or dienophiles in varying combinations may be delivered to a cell surface for iterative or simultaneous postfunctionalization via bio-orthogonal ligation reactions.

We have also been able to perform liposome fusion to the same cells several times, which may be important to tailor the membrane with multiple groups or to increase the concentration of a particular surface functional group. By rewiring cell adhesion, a number of materials, surfaces, nanoparticles, and biomedical devices for various biotechnological applications may be decorated with cells. Since no biomolecules are used with this strategy, no long-term stability and degradation issues in complex cell culture media or *in vivo* will affect cell targeting or cell assembly. Combining this strategy with polymer scaffolds, 3D tissues and organs may be generated for paracrine signaling studies, tissue replacement therapies, stem cell plasticity studies, or as a model platform for various high-throughput screening studies.[39−42] Finally, integrating this strategy with traditional liposome delivery, where the interior of the liposome contains small molecules or nanoparticle cargoes, a multiplex system with the delivery of reagents to the interior of cells and simultaneous labeling of the exterior of the cells may be possible for entirely new diagnostic and biomedical applications.

EXPERIMENTAL SECTION

All chemical reagents were of analytical grade and used without further purification. Lipids egg palmitoyl-oleoyl phosphatidylcholine (POPC) and 1,2-dioleoyl-3-trimethylammonium-propane (DOTAP) were purchased from Avanti Polar Lipids (Alabaster, AL). Antibodies and fluorescent dyes were obtained from Invitrogen (Carlsbad, CA). Trypan blue viability dye was obtained from Hyclone (Fisher Scientific, Pittsburgh, PA), and all other chemicals, including dodecanone, were obtained from Sigma-Aldrich or Fisher. Swiss 3T3 albino mouse fibroblasts (fb) were obtained from the Tissue Culture Facility at the University of North Carolina (UNC). Rat2 fb transfected with m-cherry were obtained from the Bear Lab (UNC Chapel Hill, NC). Human Mesenchymal stem cells (hMSCs) were purchased from Lonza (Basel, Switzerland).

Syntheses. Tetra(ethylene glycol)-terminated alkanethiol (EG_4)[33] and rhodamine-oxyamine (rhod-oxyamine, **4**)[43] were synthesized as previously reported. The synthesis[44] and proton nuclear magnetic resonance (^{1}H NMR) characterization of *O*-dodecyloxyamine (**A**) is presented in Supporting Information (Scheme S1).

Liposome Preparation. To generate keto- (**1**) and oxy-LUVs (**2**), dodecanone (55 μL, 10 mM solution in $CHCl_3$ at 5 mol %) and alkane-tethered oxyamine (60 μL, 10 mM solution in $CHCl_3$ at 5 mol %) were dissolved with egg-POPC (424 μL, 10 mg/mL in $CHCl_3$ at 93 mol %) and 1,2-dioleoyl-3-trimethylammonium-propane (DOTAP, 10 μL, 10 mg/mL in $CHCl_3$ at 2 mol %) in chloroform followed by concentration under high vacuum for 4 h. The dried lipid samples were then reconstituted and brought to a final volume of 3 mL in PBS buffer, pH 7.4. The contents of the vial were warmed to 50 °C and sonicated for 20 min, in a tip sonicator, until the solution became clear, and LUVs containing ketone or oxyamine groups were formed.

Rewiring Cell Adhesion. Briefly, mixed self-assembled monolayers (SAMs) presenting oxyamine (OA) or aldehyde (Ald) and EG_4 groups were patterned using microfluidic lithography[31] and microfluidic oxidation,[32] respectively. The OA and Ald group percentages were minimal (1/9 OA/EG_4, 1 mM in EtOH total) to ensure resistance to nonspecific protein and cell adhesion. Swiss 3T3 albino mouse fbs were separately cultured with keto- (**1**) or oxy- (**2**) LUVs, as previously described, and were then seeded ($\sim 10^4$ cells/mL) to surfaces patterned with OA or Ald, respectively. Over the course of 4 days, the cells adhered, spread, and proliferated, filling out the patterned regions of the surface due to the interfacial oxime reaction. The cells that were cultured with liposomes not containing the key functional groups did not attach to the patterned surfaces. The substrates were stained (see staining procedure below) and imaged by fluorescence microscopy. An exposure time of 400 and 1200 ms was used to image nuclei and actin, respectively.

Cell-Surface Reaction to Ketone-Presenting Cells. Fbs were incubated with the keto-LUVs (**1**) for 4 h and washed with PBS (4 × 25 mL), followed by addition of rhod-oxyamine (**4**, 7 mM in H_2O, 100 μL added to 4 mL) dye and incubation for 2 h. The cells were then washed with PBS (4 × 4 mL) and removed with a solution of 0.05% trypsin and 0.53 mM EDTA and resuspended in serum-free medium ($\sim 10^4$ cells/mL). The cells were then seeded to a fibronectin-coated surface for 2 h. After 2 h, serum-containing media was added for cell growth and imaged after 3 days. Phase contrast and fluorescent imaging was performed and processed using a Nikon TE2000-E inverted microscope and Metamorph software, respectively.

Flow Cytometry. Fluorescence-activated cell sorting (FACS) analysis was performed to quantify the approximate number of ketone and oxyamine groups at the cell surface after membrane fusion. Liposomes (**1**) were prepared as described above and were delivered to fbs in culture (3 mM in tris buffer, 400 μL added to 4 mL, 12 h). A time course assay was also conducted using FACS to determine whether the chemistry was being carried on after cell growth and division. Fbs (**3**) were reacted with hydrazine-conjugated biotin (3 mM in CBS, 1 mL added to 4 mL CBS in cell culture, 1 h) after culture with ketone-containing liposomes (**1**) for 1, 3, 5, and 7 days, followed by fluorescein-conjugated streptavidin (1 mM in CBS, 0.5 mL added to 4 mL CBS in cell culture, 1 h). A control cell population (not displaying ketone groups) was only incubated with biotin-hydrazide and streptavidin-fluorescein for 1 h each, under the same conditions. The cells were then centrifuged (5 min, 1000 rpm), resuspended in RPMI (without phenol red), centrifuged (5 min, 1000 rpm), and resuspended in RPMI ($\sim 10^7$ cells/2 mL). Fluorescence measurements were calibrated using RCP-5-30 beads ($\sim 10^7$ beads/mL, Spherotech, Inc., Lake Forest, IL) of

known fluorescein equivalent molecule density. Fluorescent intensities based on number of cells counted were compared to the standard bead and control cells lacking fluorescent molecule conjugation and approximate numbers of fluorescent compound bound to the surface were calculated. Flow cytometry was performed using a Dako CyAn ADP (Beckman-Coulter, Brea, CA), and data was analyzed with Summit 4.3 software.

3D Spheroid Generation. Keto- (**1**) and oxy-LUVs (**2**) were added to two separate fb populations in culture (3 mM in tris buffer, 400 μL added to 4 mL, 12 h), resulting in fusion and display of ketones and oxyamines from the cell surface. Oxyamine-presenting Rat2 fb (**5**) contained an m-cherry label (nucleus) for enhanced visualization, while the ketone-presenting Swiss 3T3 albino mouse fb (**3**) contained no fluorescent label. These two cell populations were then trypsinized and mixed together ($\sim 20^4$ cells/mL, 4 mL total) in serum containing (10% CBS, pH of 7.4) media in a 10 mL-flask and incubated at 37 °C and 5% CO_2 for 3 h. After mixing, the cells were seeded on a glass surface ($\sim 20^4$ cells/mL, 1 mL) and visualized under a Nikon TE2000-E inverted microscope or by scanning electron microscopy. Image acquisition and processing was performed using Metamorph software. An exposure time of 75 ms was used to image all spheroids.

Scanning Electron Microscopy (SEM) of 3D Spheroids. Spheroids were assembled in solution (reaction for 3 h as described above), delivered to a glass slide ($\sim 20^4$ cells/mL, 1 mL, 0.8 × 0.8 cm^2), and then fixed with 10% formalin in PBS for 15 min. The substrate was then washed with water (15 min), and cells were then dehydrated stepwise in 30, 50, 70, 90, and 100% ethanolic solutions for 15 min each. After critical point drying and sputtering 2 nm of gold, the sample was ready for imaging using a Hitachi S-4700 field emission scanning electron microscope (Hitachi High Technologies America, Inc., Schaumburg, IL).

Fibroblast Culture. Swiss 3T3 albino mouse fb and Rat2 fb were cultured in Dulbecco's Modified Eagle Medium (Gibco) containing 10% calf bovine serum (CBS) and 1% penicillin/streptomycin at 37 °C in 5% CO_2.

Human Mesenchymal Stem (hMSC) Cell Culture. hMSCs and basic, growth, and differentiation media were obtained from Lonza (Basel, Switzerland). hMSCs were cultured in Dulbecco's Modified Eagle Medium (Gibco) containing 10% fetal bovine serum (FBS) and 1% penicillin/streptomycin at 37 °C in 5% CO_2. Culturing with induction medium as described in the Lonza protocol induced Adipogenic differentiation.

Immunohistochemistry. After the growth of 3D tissue-like structures and co-culture with Swiss 3T3 albino mouse fb, surfaces were fixed with formaldehyde (4% in PBS, 30 min). Substrates were then immersed in a solution containing water and 60% isopropyl alcohol (3−5 min), followed by staining with Oil Red O (5 min) and Harris Hemotoxylin (1 min) (6,7). Substrates were visualized by phase contrast microscopy using a Nikon TE2000-E inverted microscope. Image acquisition and processing was performed using Metamorph software. An exposure time of 75 ms was used to image all HMSCs.

Directed 3D Tissue-Like Multilayers. Ketone-functionalized fbs (**3**) were seeded ($\sim 10^4$ cells/mL) to microcontact printed patterned (1 mM hexadecanethiol in EtOH, printed on gold 5 s, backfilled with 1 mM EG_4 in EtOH, 16 h) surfaces presenting fibronectin (10 mg/mL, 2 h) for 2 h. The cells were allowed to grow for 3 days (37 °C in 5% CO_2).[29] Oxyamine-functionalized fbs (**6**) ($\sim 10^4$ cells/mL) were then seeded to surfaces for 2 h, followed by addition of serum-containing (10% CBS) media to promote cell growth. The cells were cultured for 3 more days before imaging. After generation, substrates were fixed, stained, and imaged by confocal microscopy as described below.

Cell Staining for Imaging. Cells were fixed with formaldehyde (4% in PBS) and permeated (PBS containing 0.1% Triton X-100). A fluorescent dye mixture, containing phalloidin-TRITC (actin) and DAPI (nucleus) was then made in PBS containing 5% normal goat serum and 0.1% Triton X -100. Cells were incubated with the dye solution for 2 h. The substrates were then secured in fluorescence mounting medium (Dako, Carpinteria, CA), which enhances the visualization of cells when viewed under a fluorescent microscope on a glass coverslip. An exposure time of 400 and 1200 ms was used to image nuclei and actin, respectively.

Confocal Microscopy. Cell clusters and tissue formation were visualized with a Nikon Eclipse TE2000-E inverted microscope (Nikon USA, Inc., Melville, NY). The data were recorded using Leica software and a spectral confocal microscope (LeicaMicrosystems, Bannockburn, IL). An average of 84 image scans was used to generate the 3D reconstructions with Volocity software.

3D Co-culture Spheroid and Multilayer Generation. *Spheroids.* Keto- (**1**) and oxy-LUVs (**2**) were generated as previously reported, added to hMSCs and fbs (3 mM in tris buffer, 400 μL added to 4 mL, 12 h), respectively, and were cultured, resulting in fusion and display of ketones and oxyamines from the cell surface. These two cell populations were then trypsinized and mixed together in serum containing (10% FBS, pH of 7.4) media in a 10 mL flask and incubated at 37 °C and 5% CO_2 for 1, 2, 3, and 5 h. After mixing for the allotted time, cells were seeded onto a glass surface and visualized under a Nikon TE2000-E inverted microscope under the brightfield setting (75 ms exposure time). Controls were also performed where hMSCs displaying ketone groups were co-cultured with fbs (not displaying oxyamine groups) for each of the corresponding time points, 1, 2, 3, and 5 h, seeded onto glass, and imaged under the brightfield setting (75 ms). Image acquisition and processing was performed using Metamorph software.

Multilayers. Keto- (**1**) and oxy-LUVs (**2**) were added to hMSC and fbs (3 mM in tris buffer, 400 μL added to 4 mL, 12 h), respectively, and were cultured, resulting in fusion and display of ketones and oxyamines from the cell surface. hMSCs (**7**) displaying ketone groups were trypsinized and cultured on glass slides (10^5 cells/mL) and allowed to grow for 2 days. Fbs presenting oxyamines (**6**) were then trypsinized and added (10^5 cells/mL) to the hMSCs. These cells were co-cultured in media (10% FCS) for 3, 5, and 7 days, resulting in the formation of 3D multilayered, tissue-like structures of hMSCs and fbs.

Cell Viability Assay. Cell viability of 3D spheroid and multilayered tissue-like structures was assessed using a trypan blue viability assay (Hyclone, Fisher Scientific, Pittsburgh, PA). Fb spheroid and multilayer structures were prepared as previously described. A solution of 0.4% trypan blue in PBS was made and diluted in CBS (1:1) containing the spheroids (1, 3, and 5 h after mixing, 20^4 cells/mL) in solution and multilayer cell sheets (3, 5, and 7 days after a second fb population was added, 10^5 cells/mL) on a glass slide. Trypan blue was allowed to react with the cells for 2 min, at which time spheroids and surfaces were imaged and false colored with blue for enhanced visualization using a Nikon TE2000-E inverted microscope. As a control, cells were cultured for 7 days to generate a multilayer and were then fixed as mentioned above. Trypan blue was allowed to react for 2 min, and cells were imaged. For phase contrast and fluorescent imaging, exposure times of 75 and 400 ms were used, respectively.

■ ASSOCIATED CONTENT

Ⓢ Supporting Information. Additional synthetic details and ^{1}H NMR characterization of *O*-dodecyloxyamine, phase contrast and SEM images demonstrating control over composition and size of 3D spheroid formation, confocal images displaying 3D co-culture tissues with stem cells and fibroblast, and cell viability data. This material is available free of charge via the Internet at http://pubs.acs.org.

■ AUTHOR INFORMATION

Corresponding Author
mnyousaf@email.unc.edu

■ ACKNOWLEDGMENT

The authors thank Dr. Jim Bear for his generous donation of m-cherry labeled cells, Dr. Nancy Thompson and her lab group for use of equipment and expertise in liposome chemistry, Lisa Bixby for conducting FACS, and Dr. Michael Chua for aid with confocal imaging. This work was supported by the Carolina Center for Cancer Nanotechnology Excellence, the Burroughs Wellcome Foundation (Interface Career Award), and the National Science Foundation.

■ REFERENCES

(1) Nelson, C. M.; Bissel, M. J. *Annu. Rev. Cell Dev. Biol.* **2006**, *22*, 287–309.
(2) Meshel, A. S.; Wei, Q.; Adelstein, R. S.; Sheetz, M. P. *Nat. Cell Biol.* **2005**, *7*, 157–164.
(3) Isenberg, B. C.; Williams, C.; Tranquillo, R. T. *Annu. Biomed. Eng.* **2006**, *34*, 971–985.
(4) Hollister, S. J. *Nat. Mater.* **2005**, *4*, 518–524.
(5) Gillette, B. M.; Jensen, J. A.; Tang, B.; Yang, G. J.; Bazargan-Lari, A.; Zhong, M.; Sia, S. K. *Nat. Mater.* **2008**, *7*, 636–640.
(6) Tanaka, H.; Murphy, C. L.; Murphy, C.; Kimura, M.; Kawai, S.; Polak, J. M. *J. Cell Biochem.* **2004**, *93*, 454–462.
(7) Gartner, Z. J.; Bertozzi, C. R. *Proc. Natl. Acad. Sci. U.S.A.* **2009**, *106*, 4606–4610.
(8) Albrecht, D. R.; Underhill, G. H.; Wassermann, T. B.; Sah, R. L.; Bhatia, S. N. *Nat. Methods* **2006**, *3*, 369–375.
(9) Gray, D. S.; Tan, J. L.; Voldman, J.; Chen, C. S. *Biosens. Bioelectron.* **2004**, *19*, 1765–1774.
(10) Odde, D. J; Renn, M. J. *Biotechnol. Bioeng.* **2000**, *67*, 312–318.
(11) Nahmias, Y.; Odde, D. J. *Nat. Protocol* **2006**, *1*, 2288–229626.
(12) Barron, J. A.; Krizman, D. B.; Ringeisen, B. R. *Annu. Biomed. Eng.* **2005**, *33*, 121–130.
(13) Inaba, R.; Khademhosseini, A.; Suzuki, H.; Fukuda, J. *Biomaterials* **2009**, *30*, 3573–3577.
(14) Ringeisen, B. R.; Othon, C. M.; Barron, J. A.; Young, D.; Spargo, B. *J. Biotechnol.* **2006**, *1*, 930–948.
(15) Chiou, P. Y.; Ohta, A. T.; Wu, M. C. *Nature* **2005**, *436*, 370–372.
(16) Falconnet, D.; Csucs, G.; Grandin, H. M.; Textor, M. *Biomaterials* **2006**, *27*, 3044–3063.
(17) Khademhosseini, A.; Langer, R.; Borenstein, J.; Vacanti, J. P. *Proc. Natl. Acad. Sci. U.S.A.* **2006**, *103*, 2480–2487.
(18) Luo, W.; Chan, E. W. L.; Yousaf, M. N. *J. Am. Chem. Soc.* **2010**, *132*, 2614–2621.
(19) Mahal, L. K.; Yarema, K. J.; Bertozi, C. R. *Science* **1997**, *276*, 1125–1128.
(20) Prescher, J. A.; Bertozzi, C. R. *Nat. Chem. Biol.* **2005**, *1*, 13–21.
(21) Chen, I.; Howarth, M.; Lin, W.; Ting, A. Y. *Nat. Methods* **2005**, *2*, 99–104.
(22) Keppler, A.; Pick, H.; Arrivoli, C.; Vogel, H.; Jonhsson, K. *Proc. Natl. Acad. Sci. U.S.A.* **2004**, *101*, 9955–9959.
(23) Miller, L. W.; Sable, J.; Goelet, P.; Sheetz, M. P.; Cornish, V. W. *Angew. Chem. Int. Ed.* **2004**, *43*, 1672–1675.
(24) Kellam, B.; De Bank, P. A.; Shakesheff, K. M. *Chem. Soc. Rev.* **2003**, *32*, 327–337.
(25) Rabuka, D.; Forstner, M. B.; Grovers, J. T.; Bertozzi, C. R. *J. Am. Chem. Soc.* **2008**, *130*, 5947–5953.
(26) Sarkar, D.; Vemula, P. K.; Zhao, W.; Gupta, A.; Karnik, R.; Karp, J. M. *Biomaterials* **2010**, *31*, 5266–5274.
(27) Wilson, J. T.; Krishnamurthy, V. R.; Cui, W.; Qu, Z.; Chaikof, E. L. *J. Am. Chem. Soc.* **2009**, *131*, 18228–18229.
(28) Csiszar, A.; Hersch, N.; Dieluweit, S.; Biehl, R.; Merkel, R.; Hoffmann, B. *Bioconjugate Chem.* **2010**, *21*, 537–543.
(29) Dutta, D.; Pulsipher, A.; Yousaf, M. N. *Langmuir* **2010**, *26*, 9835–9841.
(30) Love, J. C.; Estroff, L. A.; Kriebel, J. K.; Nuzzo, R. G.; Whitesides, G. M. *Chem. Rev.* **2000**, *105*, 1103–1170.
(31) Lamb, B. M.; Barrett, D. G.; Westcott, N. P.; Yousaf, M. N. *Langmuir* **2008**, *24*, 8885–8889.
(32) Westcott, N. P.; Pulsipher, A.; Lamb, B. M.; Yousaf, M. N. *Langmuir* **2008**, *24*, 9237–9240.
(33) Pale-Grosdemange, C.; Simons, E. E.; Prime, K. L.; Whitesides, G. M. *J. Am. Chem. Soc.* **1991**, *113*, 12–20.
(34) Saxon, E.; Bertozzi, C. R. *Science* **2000**, *287*, 2007–2010.
(35) Hsiao, S. C.; Shum, B. J.; Onoe, H.; Douglas, E. S.; Gartner, Z.; Mathies, R. A.; Bertozzi, C. R.; Francis, M. B. *Langmuir* **2009**, *25*, 6985–6991.
(36) Mueller-Klieser, W. *Am. J. Physiol.* **1997**, *273*, C1109–C1123.
(37) Khademhosseini, A.; Vacanti, J.; Langer, R. *Sci. Am.* **2009**, *300*, 64–71.
(38) Badylak, S. F.; Nareem, R. M. *Proc. Natl. Acad. Sci. U.S.A.* **2010**, *107*, 3285–3286.
(39) Khetani, S. R.; Bhatia, S. N. *Nat. Biotechnol.* **2008**, *26*, 120–126.
(40) Zeisberg; Yang, C.; Martino, M.; Duncun, M. B.; Rieder, F.; Tanjore, H.; Kalluri, R. *J. Biol. Chem.* **2007**, *282*, 23337–23347.
(41) Bhatia, S. N.; Balis, U.; Yarmush, M. L.; Toner, M. *Biotechnol. Prog.* **1998**, *14*, 378–387.
(42) Kunz-Schughart, L. A.; Freyer, J. P.; Hofstaedter, F.; Ebner, R. *J. Biomol. Screening* **2004**, *9*, 273–285.
(43) Chan, E. W. L.; Yousaf, M. N. *J. Am. Chem. Soc.* **2006**, *128*, 15542–15546.
(44) Park, S.; Yousaf, M. N. *Langmuir* **2008**, *24*, 6201–6207.